DOI: 10.3901/CJME.2015.0107.007, available online at www.springerlink.com; www.cjmenet.com; www.cjme.com.cn

Force Characteristics in Continuous Path Controlled Crankpin Grinding

ZHANG Manchao and YAO Zhenqiang*

State Key Laboratory of Mechanical System and Vibration, Shanghai Jiao Tong University, Shanghai 200240, China

Received July 3, 2014; revised November 10, 2014; accepted January 7, 2015

Abstract: Recent research on the grinding force involved in cylindrical plunge grinding has focused mainly on steady-state conditions. Unlike in conventional external cylindrical plunge grinding, the conditions between the grinding wheel and the crankpin change periodically in path controlled grinding because of the eccentricity of the crankpin and the constant rotational speed of the crankshaft. The objective of this study is to investigate the effects of various grinding conditions on the characteristics of the grinding force during continuous path controlled grinding. Path controlled plunge grinding is conducted at a constant rotational speed using a cubic boron nitride (CBN) wheel. The grinding force is determined by measuring the torque. The experimental results show that the force and torque vary sinusoidally during dry grinding and load grinding. The variations in the results reveal that the resultant grinding force and torque decrease with higher grinding speeds and increase with higher peripheral speeds of the pin and higher grinding depths. In path controlled grinding, unlike in conventional external cylindrical plunge grinding, the axial grinding force cannot be disregarded. The speeds and speed ratios of the workpiece and wheel are also analyzed, and the analysis results show that up-grinding and down-grinding occur during the grinding process. This paper proposes a method for describing the force behavior under varied process conditions during continuous path controlled grinding, which provides a beneficial reference for describing the material removal mechanism and for optimizing continuous controlled crankpin grinding.

Keywords: grinding, torque, force, crankshaft, crankpin

1 Introduction

Crankshafts are key components of engines. Turning, milling, grinding, and broaching can be used to process crankshafts. Grinding is one of most important and preferentially used finishing processes achieving high dimensional accuracy and surface finish which plays an important role in the automotive industry[1]. Because of the special nature of the construction of crankshaft, the conventional grinding method by which a crankpin is processed involves the crankshaft being held in place by offsetting chucks to align the crankshafts pins with the main axis. Using this method, a crankpin is processed as a centered circle[2]. However, grinding of the main journals and the pin journals of a crankshaft cannot be accomplished in a single clamping operation. With increased demands for high productivity, continuous path controlled grinding process has been developed to machine non-round shaped parts such as square, rectangular, camshaft and crankshaft allowing reduction of non-productive time and re-clamping inaccuracies[3−4]. Fig. 1 illustrates the concept of continuous path controlled grinding[5]. The pin journal rotates around the C axis followed by horizontal movement of the wheelhead along the X axis. All of the main journals and pin journals of a concentrically clamped crankshaft can be ground in one setup that improves the efficiency and clamping accuracy of the process.

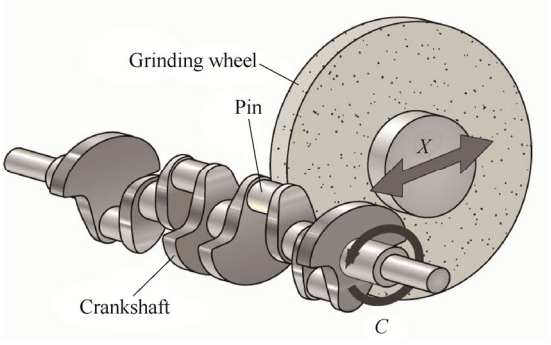

Fig. 1. Continuous path controlled crankpin grinding

The grinding force is one of the most important parameters considered which includes relevant process information during grinding. The workpiece machinability, wheel wear, chatter, geometric accuracy and surface quality of workpiece are closely related to the grinding force[6]. Research has shown that 75% of the roundness error is due to the error motion of the spindle and most of the remainder

* Corresponding author. E-mail: zqyao@sjtu.edu.cn

Supported by National Science and Technology Major Project of China (Grant No. 2013ZX04002-031), Foundation for Innovative Research Groups of the National Natural Science Foundation of China(Grant No. 51121063), and State Key Laboratory of Mechanical System and Vibration of China(Grant No. MSV2D201412)

is due to the forced vibration of the grinding wheel on the cylindrical grinding machine[7]. Evaluation of the grinding force is essential to quality control and optimization of the grinding process. Therefore, an accurate understanding of the grinding force during the crankpin grinding process has practical significance.

The effects of the process parameters, wheel properties, cooling and dressing on grinding force have been investigated experimentally[8−11]. Models for predicting tangential and normal grinding forces have also been developed for cylindrical grinding[12−13]. Such models are only applicable to the specific conditions for which they are established. WALSH, et al[2, 14−15], presented a force model based on the unique geometric characteristics of the crankshaft, grinding parameters and machine system for eccentric chuck crankpin grinding which can be regarded as conventional cylindrical plunge grinding. MÖHRING, et al[16], evaluated the influence of cutting speed, feedrate and low rate peripheral work speed on the grinding force. Moreover, DENKENA, et al[17], predicted the fluid pressure force by means of an empirical model, and also developed a model for the grinding force based on the equivalent chip thickness and the contact length. It should be noted that this model is only valid for the range of parameter values for which it was developed. Little research has been focused on continuous path controlled grinding of crankshafts.

There have been some researches on the measuring of force involved in external cylindrical grinding in the past years. Surface grinding force is readily measured using instrumentation, whereas measurement of cylindrical plunge grinding force is relatively complicated because of the effect of spindle rotation[18]. The grinding force can be obtained using the calibrated output of strain gages, piezoelectric crystals, power, pressure sensors, and displacement sensors, such as LVDTs and capacitance probes[19]. The tangential force can be obtained indirectly by calculating the measured power and wheel speed used by the operation[8, 20], but the normal grinding force cannot be obtained in this way. In a previous study, a dynamometer was constructed with four three-axis force transducers at the corners of a platform that supports two bearings in which the workpiece and its shaft are mounted[21]. The more popular approach is a sensor-based support centers with four electrical resistance strain foils pasted onto the surface[22]. The measurement systems mentioned above require professional and sophisticated skills and lead to the reduction of machine tool stiffness. A commercial rotation dynamometer for measurement of force and torque in a rotational workpiece has recently been developed[9].

An optimized strategy for continuous path controlled crankpin grinding has been presented in previous studies[23−25]. However, twin independent wheelheads are typically employed simultaneously to grind main journals and pin journals in the automotive industry. The crankshaft rotational speed is typically constant when two wheelhead units are used to machine a crankshaft. The grinding point on the wheel in contact with the eccentrically rotating pin journal moves along the surface of both the pin journal and the wheel simultaneously. The contact conditions between the wheel and crankshaft change periodically during the grinding process[26]. As a result, the magnitude and direction of the grinding force varies with respect to the phase angle of the crankshaft, unlike in conventional external cylindrical plunge grinding, in which the direction of the grinding force does not change.

This study was conducted using a methodology based on torque to investigate the effects of grinding parameters on the crankpin grinding force. The results obtained provide a good fundamental understanding of the behavior of the force induced by continuous path controlled grinding for certain grinding conditions.

2 Analysis of Crankpin Path Controlled Grinding

The mechanism of path controlled crankpin grinding is depicted in Fig. 2. The pin journal rotates around the main axis eccentrically, and the location of the wheel carriage is coupled to the rotational angle of the crankshaft. Three Cartesian coordinate systems are employed in describing this behavior. One is a global workpiece coordinate system (XO_1Y); one is a local moving coordinate system (UPV), which is attached to the grinding point P; and one is a local coordinate system (O_1O_3K) which is attached to the crankpin center O_3. The rotational angle φ is assumed to be zero when the grinding point P is located on the positive X axis. The speeds of the grinding points of the pin journal and the wheel are given with respect to the main axis rotational angle φ as follows:

$$\beta = \arcsin\frac{R_o \sin\varphi}{R_p + R_s}, \tag{1}$$

$$\delta = \arctan\frac{R_s \sin\beta}{R_o \cos\varphi + R_p \cos\beta}, \tag{2}$$

$$O_1P = \sqrt{(R_o \cos\varphi + R_p \cos\beta)^2 + (R_s \sin\beta)^2}, \tag{3}$$

$$V_{wu}(\varphi) = \omega O_1P \cos(\delta + \beta), \tag{4}$$

$$V_{su}(\varphi) = V_x \sin\beta + V_s, \tag{5}$$

where φ is the rotational angle of the crankshaft, R_o is the eccentricity of the crankpin, R_s is the wheel radius, R_p is the radius of the pin journal, $V_{wu}(\varphi)$ is the crankpin tangential speed along the U axis, $V_{su}(\varphi)$ is the wheel tangential speed along the U axis, ω is the angular speed of the main axis, and V_s is the substantial wheel speed.

The speed characteristics of the grinding point and the grinding speed ratio are plotted in Fig. 3 as a function of the rotational angle φ for R_p=40 mm, R_o=67.5 mm,

R_s=300 mm, V_s=90 m/s, V_w=35 r/min, a_p=0.01 mm in Fig. 2. The speed ratio k_v is defined as $V_{wu}(\varphi)/V_{su}(\varphi)$. Depending on the speed ratio, there are two modes during path controlled crankpin grinding: up-grinding and down-grinding. The two modes alternate during one revolution.

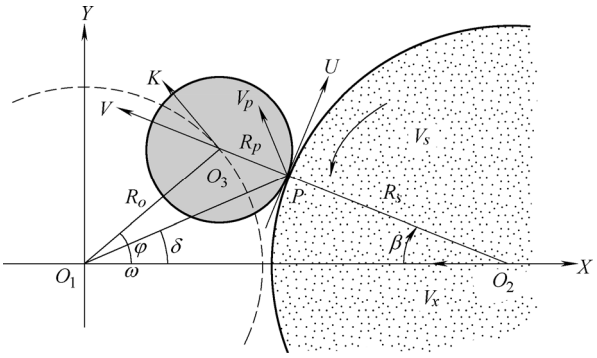

Fig. 2. Kinematics of path controlled grinding of crankpin

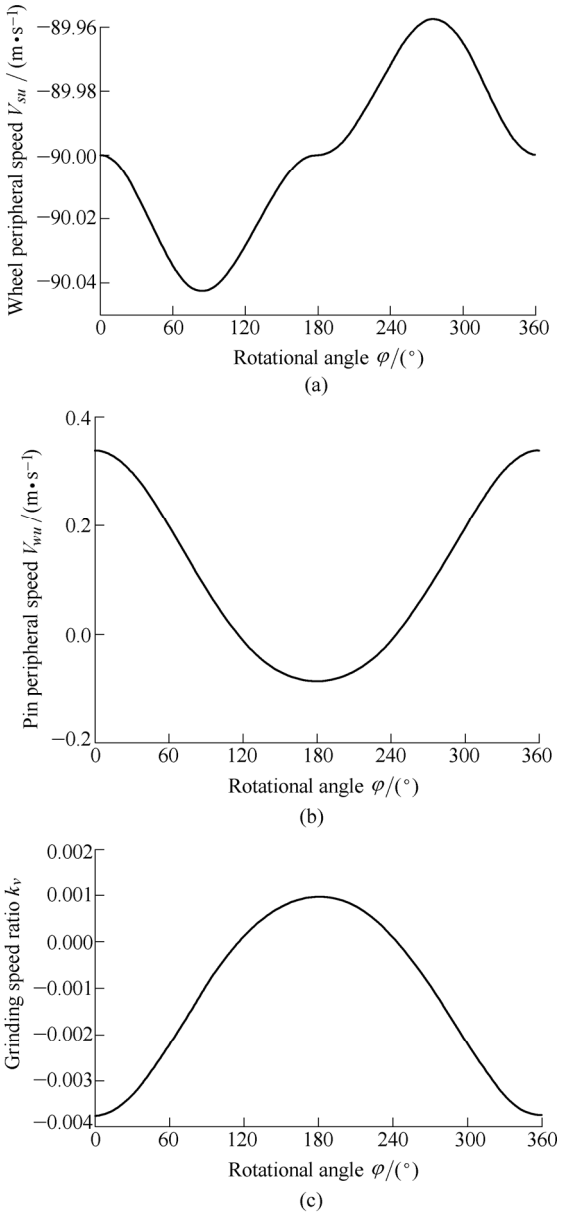

Fig. 3. Analysis of speed and speed ratio for the pin journal and wheel

3 Experiments Procedure

Grinding was conducted under flood emulsion cooling, and the hydraulic pressure was set to 0.39 MPa. The water-based solution was diluted by the ratio of 1:15. The nozzle setup of the coolant maintains a settled location. The continuous path controlled grinding setup is shown in Fig. 4. Each test consisted of at least ten revolutions during dry run and at least ten revolutions during grinding, so that the signals produced were sufficient to obtain information on the force characteristics during grinding. The grinding conditions employed in this study are shown in Table 1.

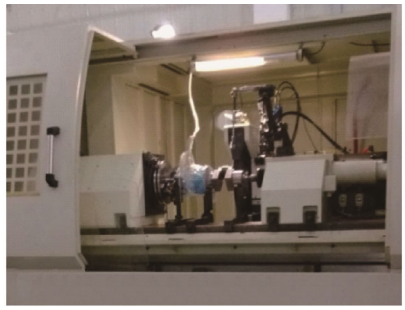

(a) Machined setup

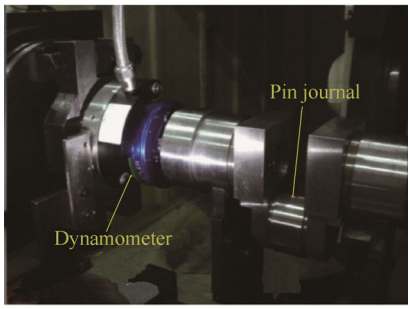

(b) Machined workpiece

Fig. 4. Experiment setup

Table 1. Experimental conditions

Parameter	Value
Wheel	CBN(φ600)
Wheel speed V_s/(m • s^{-1})	75, 85, 90, 95
Grinding depth a_p/mm	0.005, 0.01,0.015
Rotational speed n/(r • min^{-1})	15, 25, 30, 35, 50
Dresser	Diamond roller dresser (φ135)
Wheel speed v/(m • s^{-1})	30
Dressing speed v_d/(m • s^{-1})	24
Dressing depth h/mm	0.003
Dressing feed a/(mm • min^{-1})	200

A pin journal of 40Cr steel was designed, fabricated, and heated to hardness of HRC 52±3. The initial dimensions of the pin journal were 80 mm (diameter)×35 mm (width). The pin journal was assembled to crank web at an eccentricity of 67.5 mm. The CBN grinding wheel used had an initial diameter of 600 mm and a width of 38 mm (Komm-Nr.0701 0100 1/1 3b 126×26 V8118-150, KREBS&RIEDEL Inc., Germany), and was dressed prior to each test using a diamond roller dresser with a diameter

of 150 mm (KUNTZ Inc., Germany) to ensure similar grinding wheel conditions in those tests.

A four-component rotational dynamometer (Kistler 9123C), the performance parameters of which are listed in Ref. [27], was employed to measure the grinding force and torque. The dynamometer was fixed on the crankshaft as an assembled part mounted between the headstock and the tailstock. The sample frequency was 8192 Hz. The measurement signals were recorded on a laptop computer using the LMS SCADAS Mobile SCM05 data acquisition system and the LMS Test.lab V10b software.

4 Results and Discussion

4.1 Torque characteristics during grinding

The torque dependent on grinding parameters and crankshaft rotational angle are important to the accuracy of the surface. For the cases considered in this study, the trends of the torque M are very similar. A typical torque profile of torque is shown in Fig. 5. It is seen that the torques vary sinusoidally during unloaded grinding and loaded grinding.

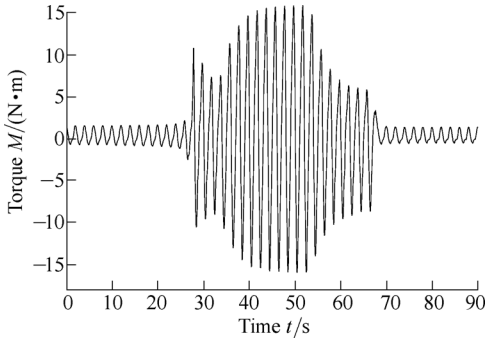

Fig. 5. Typical curve of torque under constant rotational speed during grinding

The net grinding torque M_{net} can be determined by subtracting the dry run torque from the grinding torque. To obtain an estimate of the torque, data smoothing based on an exponential smoothing method with a factor of 0.95 was accomplished using the LMS Test.lab V10b software. Fig. 6 shows the net grinding torque acting on the crankshaft for various combinations of parameters. It appears that resultant grinding torque decreases with higher grinding speed, increases with higher peripheral speed of pin journal and higher grinding depth for large range of revolution. These variations are not just the result of the workpiece speed and wheel variation. As noted earlier, the grinding point speed and the location on the wheel and pin journal change along the surface simultaneously. The force components along the O_1 axis and the K axis reflect the partial normal grinding force and the partial tangential grinding force simultaneously.

As Fig. 6 shows, it is known that the maximum torque occurs at wheel speed 75 m/s, crankshaft rotational speed 50 r/min and grinding depth 0.015 mm. The minimum torque exists under given conditions wheel speed 90 m/s, crankshaft rotational speed 20 r/min and grinding depth 0.005 mm. In other words, the maximum and the minimum forces exhibit at the same location on the K axis. In addition, it exhibits the maximum torque at one location, whereas at other locations, the variation of the torque is gentle. Zero torque is also found during the crankpin grinding. However, the locations of the extreme values of the torque are not the same. For this reason, because of the torsional stiffness of the crankshaft, the vibration and the variation in force, the actual position of the crankshaft may be slightly different from the theoretical position[28].

To evaluate the effects of grinding parameters on the grinding force as well as quantitative values of the grinding force, it is assumed that the moment arm is equal to the eccentricity of the crankpin. The variation of the force along the K axis is plotted in Figs. 6(d), 6(e), and 6(f). These profiles intuitively indicate that the force decreases with the increase of wheel speed, increases with the increase of workpiece speed and grinding depth.

In order to evaluate the relationship between the grinding parameters and the grinding force, the grinding force at 0° and 180°, at which only the tangential grinding force contributes to the measured torque, was investigated, as shown in Fig. 7. It is seen that the force decreases with an increase of wheel speed and increases with an increase of rotational speed and grinding depth increase. Previous studies have shown that the grinding force is dependent on the maximum undeformed chip thickness h_{max}. The influence of the grinding conditions on the grinding force can be explained in terms of the maximum undeformed chip thickness. A smaller value of h_{max} results in a lower force. The maximum undeformed chip thickness can be expressed as follows[29]:

$$h_{max} = \left(\frac{3}{c\tan\alpha}\right)^{0.5}\left(\frac{V_{wu}}{V_{su}}\right)^{0.5}\left(\frac{a_p}{d_s}\right)^{0.25}, \qquad (6)$$

where C is the density of the active cutting points, α is the semi-included angle for the undeformed chip cross section, and d_s is the wheel diameter.

The grinding thickness of a single grain is reduced with the wheel speed increase. In addition, with increase of the grinding wheel speed, the more heat generated in the grinding zone softens the metal[8]. As a result, the grinding force decreases with an increase of wheel speed. As expected, increasing the grinding depth and the workpiece speed increases the maximum undeformed chip thickness. With increase of rotational speed of crankpin, more workpiece material per unit time needs to be machined which leads to an increase of the grinding force. As the grinding depth increases, more grains participate in cutting, and the chip deformation and friction between the grain and the workpiece increase. Therefore, the grinding force increases with more grains participates in grinding[30].

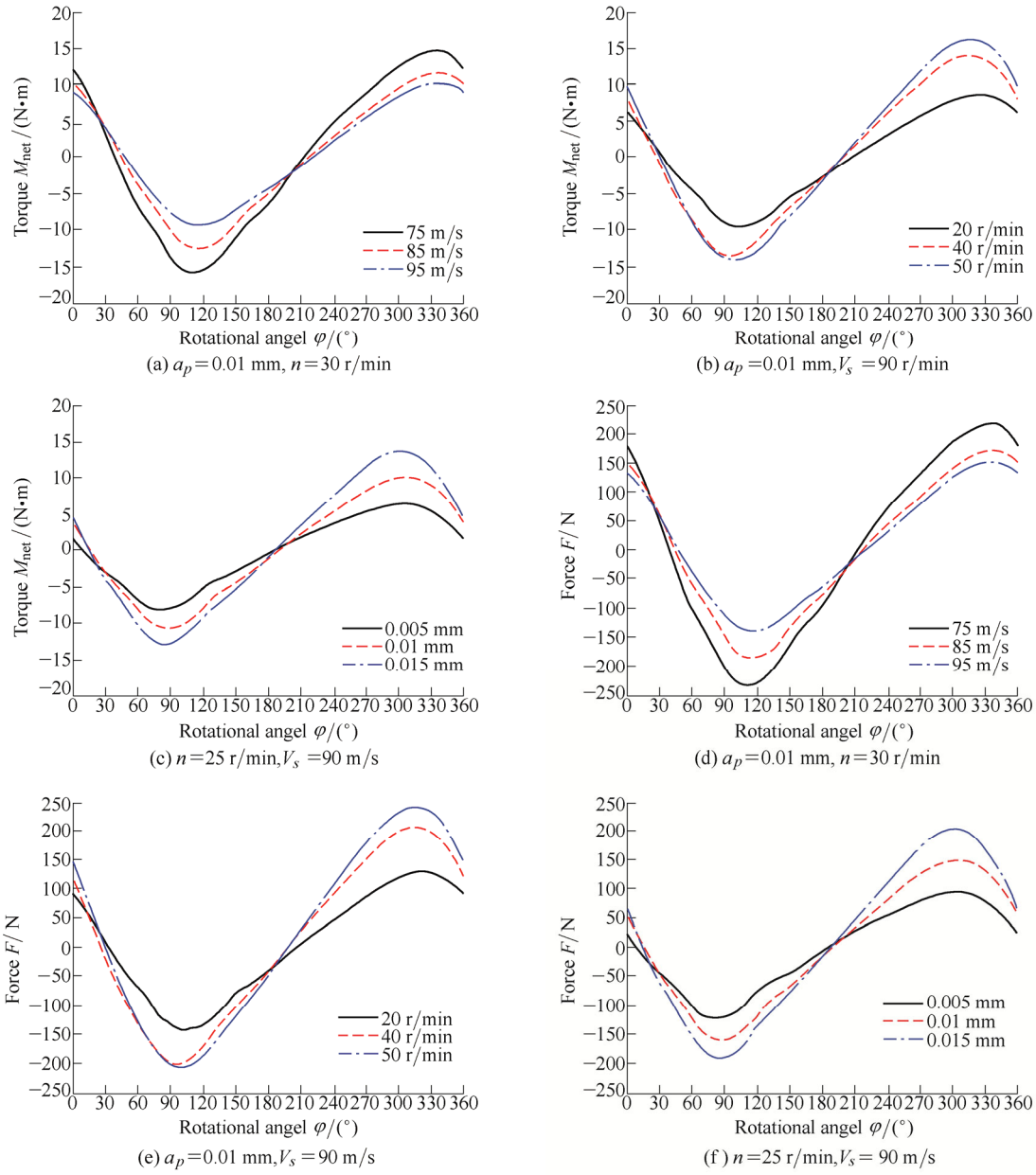

Fig. 6. Torque and force profiles for different grinding conditions

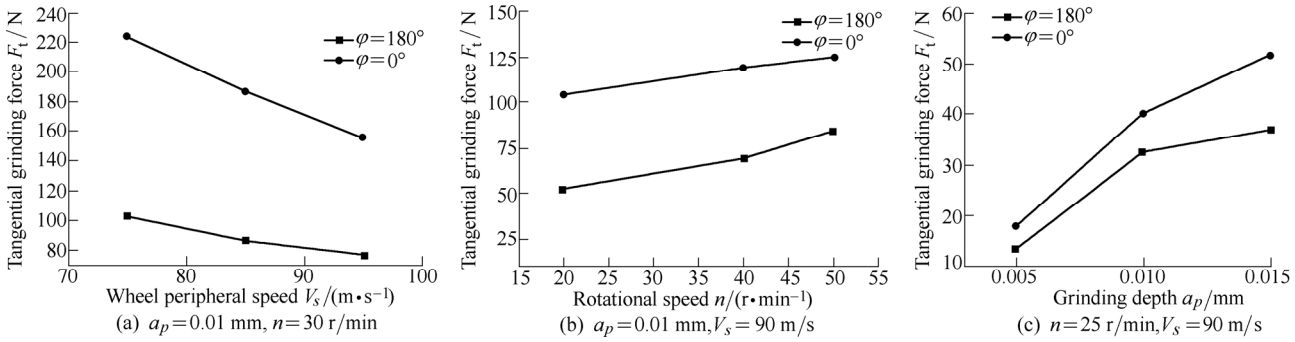

Fig. 7. Tangential grinding force at 0° and 180°

On the other hand, it can also be observed that the tangential grinding forces at 180° are greater than those at 0°. The chip thickness is changed from large to small in down-grinding, and from small to large in up-grinding, which results in the difference between the two grinding modes[31]. The grinding force can be divided into cutting force, and sliding force. The sliding forces increase proportionally with wear flat area whilst the cutting forces remain constant[32]. A short chip length and a large undeformed chip thickness are produced in up-grinding; therefore, the sliding force is smaller than the cutting force. During down-grinding, a greater grinding force occurs

because of the greater sliding force[33].

4.2 Forces characteristics during grinding

The measured force and torque curves for the test conditions exhibit similar trends. To understand the force characteristics during crankpin grinding, the profiles of force and torque are presented corresponding to the grinding time using the parameter wheel speed 75 m/s, crankshaft rotational speed 30 r/min and grinding depth 0.01 mm as shown in Fig. 8. In The graph shows five revolutions during grinding in which every peak means a single revolution of crankshaft. The periods exhibit similar trends and repeat in accordance with the test conditions.

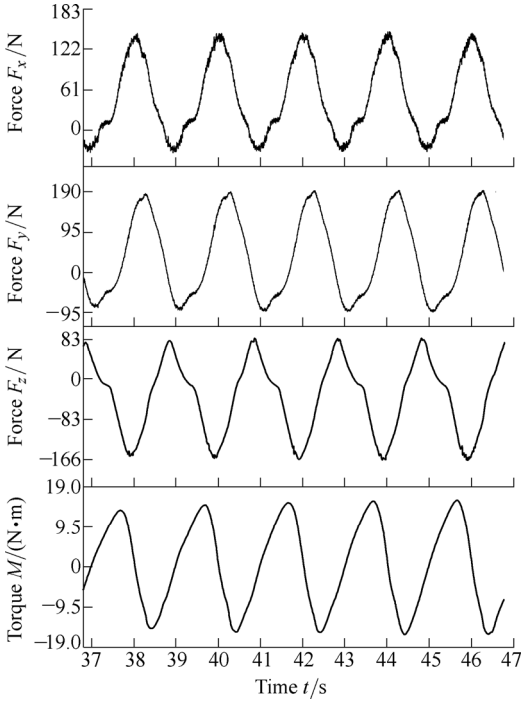

Fig. 8. Distribution of force and torque during grinding

It can be observed that the forces F_x, F_y, and F_z are all dominant forces during continuous path controlled crankpin grinding. The forces F_x, F_y, and F_z denote the gravitational, centrifugal and grinding forces respectively, with respect to the rotary dynamometer's built-in coordinate system. It is clear that the forces vary during grinding which means that it would cause torsional vibration[31]. Although the curve of the speed ratio is smooth, it should be noted that the force and torque do not exhibit the same smooth variation.

Fig. 9 presents the distribution of the net grinding force during crankpin cylindrical plunge grinding for wheel speed 75 m/s, crankshaft rotational speed 30 r/min and grinding depth 0.01 mm. It is found that the forces F_x, F_y, and F_z are all larger. The effect of the axial grinding force F_z cannot be disregarded, which is not the case with external circle cylindrical plunge grinding. Moreover, it indicates that the forces are not same values by comparison to the force in Fig. 6 and Fig. 9. This is due to that it exist certain angle between the built-in coordinate system of the rotary dynamometer and the local coordinate system (O_1O_3K) as shown in Fig. 2.

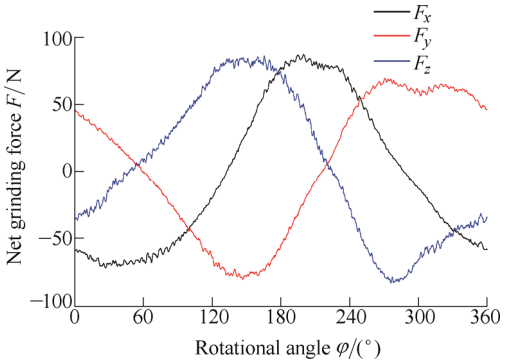

Fig. 9. Distribution of net grinding force

5 Conclusions

(1) Two kinds of grinding mode occur during continuous path controlled crankpin grinding process at one revolution: up-grinding and down-grinding. Up-grinding occurs during two thirds of the grinding process.

(2) The results of the tests conducted indicate that the grinding force and torque vary sinusoidally during dry run grinding and load grinding.

(3) The effect of the axial grinding force is significant and cannot be disregarded, unlike in external circle cylindrical plunge grinding.

References

[1] WALSH A P, BALIGA B, HODGSON P. A novel technique to optimize grinding processes[C]//*Proceedings of the International Manufacturing Leaders Forum, Leadership of the Future in Manufacturing*, Australia, February 8−10, 2002: 101−106.

[2] WALSH A. *Mathematical modelling of the crankshaft pin grinding process*[D]. Geelong, Victoria, Australia, Deakin University, 2004.

[3] TÖNSHOFF H K, KARPUSCHEWSKI B, MANDRYSCH T, et al. Grinding process achievements and their consequences on machine tools challenges and opportunities[J]. *CIRP Annals - Manufacturing Technology*, 1998, 47(2): 651−668.

[4] DRAZUMERIC R, BADGER J, KRAJNIK P. Geometric, kinematical and thermal analyses of non-round cylindrical grinding[J]. *Journal of Materials Processing Technology*, 2014, 214(4): 818−827.

[5] FUJIWARA T, TSUKAMOTO S, MIYAGAWA, M. Analysis of the grinding mechanism with wheel head oscillating type CNC crankshaft pin grinder[J]. *Key Engineering Materials*, 2005, 291−292: 63−168.

[6] TANG Jinyuan, DU Jin, CHEN Yongping. Modeling and experimental study of grinding forces in surface grinding[J]. *Journal of Materials Processing Technology*, 2009, 209(6): 2847−2854.

[7] RAO S B, COLLINS J F, WU S M. A quantitative analysis of roundness error in cylindrical chuck grinding[J]. *International Journal of Machine Tool Design and Research*, 1981, 21(1): 41−48.

[8] THIAGARAJAN C, SIVARAMAKRISHNAN R, SOMASUNDARAM S. Experimental evaluation of grinding forces and surface finish in cylindrical grinding of Al/SiC metal matrix composites[J]. *Proceedings of the Institution of Mechanical Engineers Part B: Journal of Engineering Manufacture*, 2011, 225(9): 1606−1614.

[9] TAWAKOLI T, HEISEL U, LEE D H, et al. An experimental investigation on the characteristics of cylindrical plunge dry

grinding with structured cbn wheels[C]//*5th CIRP Conference on High Performance Cutting*,Zurich, Switzerland, June 4, 2012: 399−403.

[10] MONICI R D, BIANCHI E C, CATAI R E. et al. Analysis of the different forms of application and types of cutting fluid used in plunge cylindrical grinding using conventional and superabrasive CBN grinding wheels[J]. *International Journal of Machine Tools and Manufacture*, 2006, 46(2): 122−131.

[11] WEGENER K, HOFFMEISTER H W, KARPUSCHEWSKI B, et al. Conditioning and monitoring of grinding wheels[J]. *CIRP Annals - Manufacturing Technology*, 2011, 60 (2): 757−777.

[12] LIU Qiang, CHEN Xun, WANG Yan, et al. Empirical modelling of grinding force based on multivariate analysis[J]. *Journal of Materials Processing Technology*, 2008, 203(1−3): 420−430.

[13] MISHRA V K, SALONITIS K. Empirical estimation of grinding specific forces and energy based on a modified werner grinding model[J]. *Procedia CIRP*, 2013, 8(0): 287−292.

[14] WALSH A, BALIGA B, HODGSON P D. A study of the crankshaft pin grinding forces[J]. *Key Engineering Materials*, 2004, 257−258: 75−80.

[15] WALSH A P, BALIGA B, HODGSON P D. Force modelling of the crankshaft pin grinding process[J]. *Proceedings of the Institution of Mechanical Engineers Part D: Journal of Automobile Engineering*, 2004, 218(3): 219−227.

[16] MÖHRING H C, GÜMMER O, FISCHER R. Active error compensation in contour-controlled grinding[J]. *CIRP Annals-Manufacturing Technology*, 2011, 60(1): 429−432.

[17] DENKENA B, FISCHER R. Theoretical and experimental determination of geometry deviation in continuous path controlled OD grinding processes[J]. *Advanced Materials Research*, 2011, 223: 784−793.

[18] MARSH E R, MOERLEIN A W, DEAKYNE T R S, et al. In-process measurement of form error and force in cylindrical-plunge grinding[J]. *Precision Engineering*, 2008, 32(4): 348−352.

[19] COUEY J A, MARSH E R, KNAPP B R, et al. Monitoring force in precision cylindrical grinding[J]. *Precision Engineering*, 2005, 29(3): 307−314.

[20] OLIVEIRA J F G, FRANÇA T V, WANG J P. Experimental analysis of wheel/workpiece dynamic interactions in grinding[J]. *CIRP Annals-Manufacturing Technology*, 2008, 57(1): 329−332.

[21] DREW S J, MANNAN M A, ONG K L, et al. The measurement of forces in grinding in the presence of vibration[J]. *International Journal of Machine Tools and Manufacture*, 2001, 41(4): 509−520.

[22] LI Z. C, LIN B, XU Y S, et al. Experimental studies on grinding forces and force ratio of the unsteady-state grinding technique[J]. *Journal of Materials Processing Technology*, 2002, 129(1−3): 76−80.

[23] XU Dinghong, SUN Zongyu, ZHOU Zhixiong, et al. Research on motion model of tangential point grinding[J]. *Chinese Journal of Mechanical Engineering*, 2002, 38(8): 68−73. (in Chinese)

[24] ZHOU Zhixiong, LUO Hongpoing, MI Haiqing, et al. On the tangential point tracing grinding for a crankshaft part[J]. *China Mechanical Engineering*, 2002, 13(23): 2004. (in Chinese)

[25] XU Dihong. *The research on some key technology in the tangential point tracing grinding methods*[D]. Changsha: Hunan university, 2005. (in Chinese)

[26] ÁLVAREZ J, BARRENETXEA D, MARQUÍNEZ J I, et al. Effectiveness of continuous workpiece speed variation (CWSV) for chatter avoidance in throughfeed centerless grinding[J]. *International Journal of Machine Tools and Manufacture*, 2011, 51(12): 911−917.

[27] KISTLER. *Rotating 4-component dynamometer RCD for cutting force measurement up to 10 000 1/min*[M/OL]. [2014-06-23]. http://www.kistler.com/cn/en/product/torque/9123C1011.

[28] ZHOU Zhixiong, LUO Hongpoing, XU Dihong, et al. Analysis and compensation of stiffness-error of crankshaft in tangential point tracing grinding[J]. *Chinese Journal of Mechanical Engineering*, 2003, 39(6): 98−101. (in Chinese)

[29] HUANG H, LIU Y. C. Experimental investigations of machining characteristics and removal mechanisms of advanced ceramics in high speed deep grinding[J]. *International Journal of Machine Tools and Manufacture*, 2003, 43(8): 811−823.

[30] YAO C F, JIN Q C, HUANG X C, et al. Research on surface integrity of grinding Inconel718[J]. *International Journal of Advanced Manufacturing Technology*, 2013, 65(5−8): 1019–1030.

[31] CHEN Jianyi, HUANG Hui, XU Xipeng. An experimental study on the grinding of alumina with a monolayer brazed diamond wheel[J]. *International Journal of Advanced Manufacturing Technology*, 2009, 41(1−2): 16−23.

[32] MALKIN S, COOK N H. The wear of grinding wheels (Part 1)[J]. *Transactions of ASME*, 1971, 93: 1102−1128.

[33] TSO P L. Study on the grinding of Inconel 718[J]. *Journal of Materials Processing Technology*, 1995, 55(3−4): 421−426.

Biographical notes

ZHANG Manchao, born in 1975, is currently a PhD candidate at *State Key Lab of Mechanical System and Vibration, Shanghai Jiao Tong University, China*. His main research interest is precision machining.
E-mail: sliders@163.com

YAO Zhenqiang, born in 1962, is currently a professor at *State Key Lab of Mechanical System and Vibration, Shanghai Jiao Tong University, China*.
Tel: +86-21-34206315; E-mail: zqyao@sjtu.edu.cn